Optimization of vascular structure of self-healing concrete using deep neural network (DNN)

Wan, Zhi; Chang, Ze; Xu, Yading; Šavija, Branko

DOI
10.1016/j.conbuildmat.2022.129955

Publication date
2023

Document Version
Final published version

Published in
Construction and Building Materials

Construction and Building Materials 364 (2023) 129955

Contents lists available at ScienceDirect

Construction and Building Materials

journal homepage: www.elsevier.com/locate/conbuildmat

Optimization of vascular structure of self-healing concrete using deep neural network (DNN)

Zhi Wan *, Ze Chang, Yading Xu, Branko Šavija

Faculty of Civil Engineering and Geosciences, Delft University of Technology, 2628CN Delft, The Netherlands

ARTICLE INFO

Keywords:
Concrete
Self-healing
Deep neural network
Structure optimization
Numerical simulation

ABSTRACT

In this paper, optimization of vascular structure of self-healing concrete is performed with deep neural network (DNN). An input representation method is proposed to effectively represent the concrete beams with 6 round pores in the middle span as well as benefit the optimization process. To investigate the feasibility of using DNN for vascular structure optimization (i.e., optimization of the spatial arrangement of the vascular network), structure optimization improving peak load and toughness is first carried out. Afterwards, a hybrid target is defined and used to optimize vascular structure for self-healing concrete, which needs to be healable without significantly compromising its mechanical properties. Based on the results, we found it feasible to optimize vascular structure by fixing the weights of the DNN model and training inputs with the data representation method. The average peak load, toughness and hybrid target of the ML-recommended concrete structure increase by 17.31%, 34.16% and 9.51%. The largest peak load, toughness and hybrid target of the concrete beam after optimization increase by 0.17%, 14.13%, and 3.45% compared with the original dataset. This work shows that the DNN model has great potential to be used for optimizing the design of vascular system for self-healing concrete.

1. Introduction

Concrete is the most widely-used construction material due to its good performance and relatively low price. It is a quasi-brittle material, strong in compression while relatively weak in tension, making it sensitive to crack formation [1]. Cracking is one of the main causes for deterioration of concrete structures [2]. Therefore, it is important to repair large cracks before serious problems occur. Self-healing concrete is a promising approach to crack repair ("healing") with no or little human intervention [3–5]. Compared with other kinds of self-healing concrete, vascular based self-healing concrete could continuously supply healing agent if needed [6–8]. As a result, the maximum healable crack width is larger than other kinds of self-healing concrete [9]. Besides, the self-healing process could be performed multiple times to prolong the service life of concrete structures before the inside vascular network is fully blocked [10].

For vascular based self-healing concrete, the vascular structure is of great importance for the mechanical properties (strength, stiffness) as well as for the self-healing capacity. On one hand, the embedded vascular network should not dramatically decrease the initial properties of concrete. Most of the times, load bearing (strength) is the key factor in the design of concrete structures. According to previous research [11], the presence of vascular network has an adverse influence on the initial flexural strength under 4-point bending when 3D-printed octet vascular is embedded in cementitious matrix. Besides, the shape of vascular also has great influences on the mechanical properties of concrete [12]. On the other hand, in order for the self-healing process to be triggered, the crack needs to hit the vascular [13]. Vascular materials also greatly influence the release of healing agent. In previous studies, materials such as glass [6,14,15], Polyvinyl chloride (PVC) tubes [16], or Acrylonitrile Butadiene Styrene (ABS) [11] have been used as vascular materials because of their brittleness nature. However, those brittle materials, especially glasses, may not be able to survive the casting process of concrete. Alternatively, some removable materials have been used to create hollow channels as flowing path for self-healing agent when adopting 3D printing technology to fabricate the vascular network [17–19]. Hollow tubes in networks outperform the non-removable vascular network in some aspects. First, the vascular network existing in cementitious matrix needs to be monitored for a long time. Furthermore, for a vascular self-healing system, the vascular network needs to

* Corresponding author.
E-mail addresses: Z.Wan-1@tudelft.nl (Z. Wan), Z.Chang-1@tudelft.nl (Z. Chang), Y.Xu-5@tudelft.nl (Y. Xu), B.Savija@tudelft.nl (B. Šavija).

https://doi.org/10.1016/j.conbuildmat.2022.129955
Received 10 October 2022; Received in revised form 26 November 2022; Accepted 1 December 2022
Available online 9 December 2022

rupture timely in order for the self-healing agent to be released; if a hollow tube system is used instead, this is not an issue. However, without vascular tubes, the vascular network in self-healing concrete could be regarded as a defect which lowers the load bearing capacity. In this case, mechanical properties and the self-healing capacity (i.e., the process of triggering self-healing by cracks passing through the vascular channel) seem to be contradictory. Therefore, it is essential to design the concrete with hollow channels while keeping in mind the tradeoff between those two aspects.

There are several ways to carry out optimization of concrete composites. Among others, experiments are often used. For example, different octet lattice reinforcements embedded in concrete were experimentally investigated for improving the mechanical properties [20]. Li et al [21] experimentally investigated the influence of vascular networks on the concrete strength before and after injecting sodium silicate as the healing agent. However, experiments are time-consuming and significant resources are utilized. Topological optimization based on numerical simulation is another option [22–24]. However, the design space may be extraordinarily massive when the compositional and topological structures are complex [25]. Besides, the optimization may be stuck in sub-optimal when using some gradient-based topology optimization methods. Recently, optimization with machine learning (ML) methods has been proposed in material design for computational efficiencies [26] as well as capacity of overcoming local minima [27]. Gu and her colleagues designed composite materials with better quality using generative deep neural network [28] and deep reinforcement learning [29]. To date, however, no advanced optimization approaches based on ML have been developed for vascular based self-healing concrete. When designing concrete composites with ML, it is important to properly represent the complicated material structure without adding burden to the training of ML model and optimization process. In addition, the optimization target suitable for self-healing capacity needs to be defined before the optimization process.

Herein, we show the feasibility of optimizing the vascular structure configuration of vascular-based self-healing concrete with deep neural network (DNN). The DNN is chosen as the ML algorithm for its excellent performance to tackle complex tasks [30]. The purpose of the optimization is to make the concrete healable without significantly compromising its mechanical properties by finding a certain vascular structure configuration in concrete. To map the vascular structures to the target mechanical property, a dataset is first created using a commercial numerical package Abaqus/Explicit for numerically simulating the mechanical response of concrete beams with various vascular configurations subjected to 3-point bending. The optimization constraint is that 6 pores are placed out of 40 possible positions in the middle span of the beam to act as the vascular reservoirs perpendicular to the longitudinal axis of the beam. The inputs for the DNN are represented by describing the state of the 40 positions in the design space (Section 2.1). The ML method as well as the data post-processing is then introduced in detail (Section 2.2). To verify the effectiveness of the abovementioned data representation and post-processing, vascular structure optimization aimed at a single mechanical property, i.e., higher peak load and toughness respectively, are first carried out (Section 3.2). Afterwards, a hybrid target combining peak load and toughness is defined and used to optimize vascular structure for self-healing concrete, which needs to be healable without significantly compromising its mechanical properties (e.g. strength or toughness) (Section 3.3). The vascular structure on a concrete beam before and after ML optimization are compared and conclusions are drawn based on the obtained results (Section 4).

2. Data generation and Machine learning method

To investigate the possibility of tailoring vascular structure for maximizing a certain mechanical property for self-healing concrete with ML, the mechanical response of concrete with different vascular structures is first numerically calculated to create a dataset for training the ML model. The constrain of the vascular structure is that 6 pores (diameter = 4 mm) are placed in 40 positions (with a dimension of $5mm \times 5mm$) in middle span of the concrete structure. As a result, the design space is more than 3.83 million combinations (C_{40}^{6}), which makes it unfeasible to use a brute-force approach for exploring the design space in search of the optimum. The notched concrete structures under 3-point bending are investigated since the vascular structure is relatively sensitive when the pores are located in the middle span of the beam. The schematics of the concrete beam under 3-point bending test is shown in Fig. 1.

2.1. Data generation with numerical simulation

2.1.1. Data generation with Abaqus software

When using ML for optimization, the first step is to establish the relationship between vascular structure of concrete (input) and the target mechanical property (output). Therefore, a large dataset is needed for training ML model. Numerical simulation is adopted to simulate the 3-point bending test with Abaqus software. To accelerate the computation, 2-dimensional models with plane stress are built.

Considering the excellent performance of concrete damage plasticity model (CDPM) in describing the nonlinear behavior of cementitious materials, CDPM is used to define the material properties [31]. Among other, tension stiffening and compression hardening are defined (as shown in Fig. 2). The stress–strain relations under uniaxial tension and compression loading are shown in Equation (1).

$$\sigma_t = (1-d_t)E_0\left(\varepsilon_t - \tilde{\varepsilon}_t^{pl}\right)\ \sigma_c = (1-d_c)E_0\left(\varepsilon_c - \tilde{\varepsilon}_c^{pl}\right) \tag{1}$$

whereσ_t, σ_c are the tensile stress and compressive stress, respectively;d_t,d_c are tensile damage variable and compressive damage variable ranging from 0 (undamaged) to 1 (total loss of strength). E_0 is the initial (undamaged) elastic stiffness of the material;ε_t, ε_c are the total strains;$\tilde{\varepsilon}_t^{pl}$, $\tilde{\varepsilon}_c^{pl}$ are the equivalent plastic strains. In this study, the stiffness degradation is not considered and the damage variables are set to 0. The equivalent plastic strains are equal to crack strains. As shown in Fig. 2, the crack strains ($\tilde{\varepsilon}_t^{ck}$, $\tilde{\varepsilon}_c^{ck}$) are defined as the total strain minus the elastic strain corresponding to the undamaged materials (Eq.2 ~ 3).

$$\tilde{\varepsilon}_t^{ck} = \varepsilon_t - \varepsilon_{0t}^{el} \text{ or } \tilde{\varepsilon}_c^{ck} = \varepsilon_c - \varepsilon_{0c}^{el} \tag{2}$$

$$\varepsilon_t^{el} = \sigma_t/E_0 \text{ or } \varepsilon_c^{el} = \sigma_c/E_0 \tag{3}$$

The concrete beam is vertically loaded to 0.2 mm with a speed of 0.01 mm/s. The 6 displacements of the load rollers in the bottom (support) are fixed. The 3 load rollers contact with the main concrete structure with the contact type of surface-to-surface contact (Explicit), where normal behavior is defined as “hard” contact and tangential behavior if penalty friction with a coefficient of 0.05. The mesh size in the middle part (60 mm) is chosen as 0.5 mm. It gradually changes to 5 mm from the middle to side within 10 mm, then the mesh size is kept 5 mm in the rest 40 mm (Fig. 3).

The input for CDMP for cementitious materials is listed in Table 1.

2.1.2. Data representation

It is of great importance to define the input and output when creating the dataset for ML [32]. Identifying the characterizing features is important to accelerate the training process and minimize the cost function [33]. To accelerate the training process of the ML model, the information without much variance should be removed. In this work, the concrete beam outside the design space is almost the same for all investigated vascular based self-healing concretes. Therefore, the characterization of vascular structures could be effectively represented by the design space in the middle span. The design space could be described by the state of the 40 locations, i.e., with or without a pore.

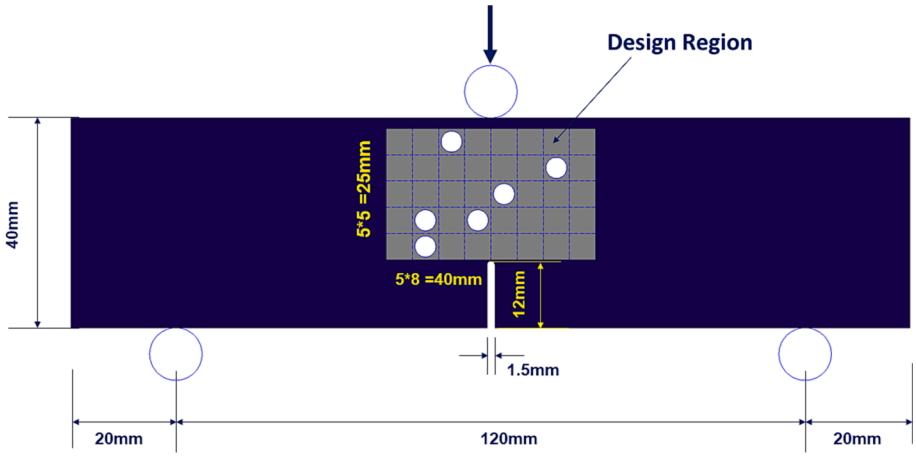

Fig. 1. Schematics of the 3-point bending test.

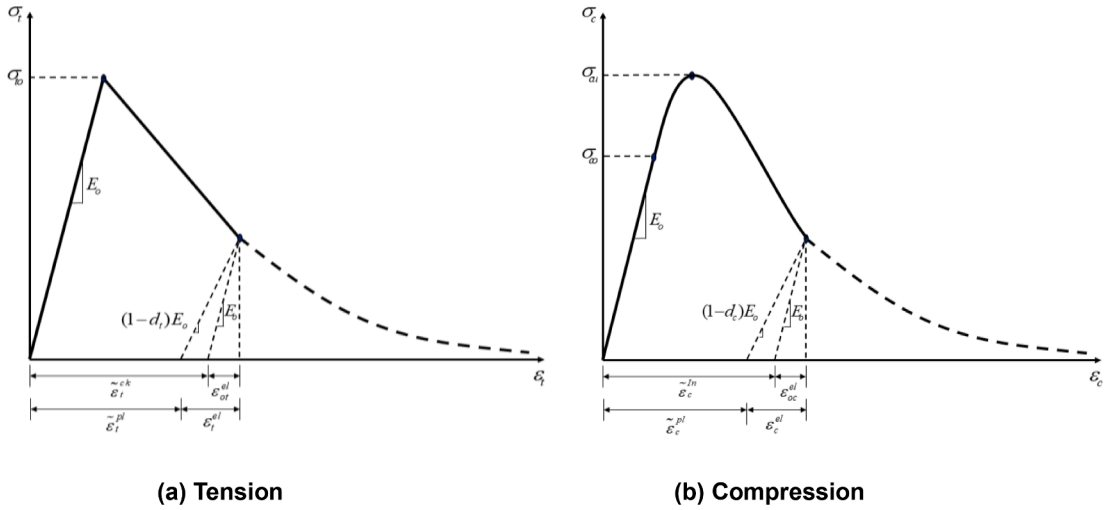

Fig. 2. Constitutive law of CDPM in (a) Tension; (b) Compression.

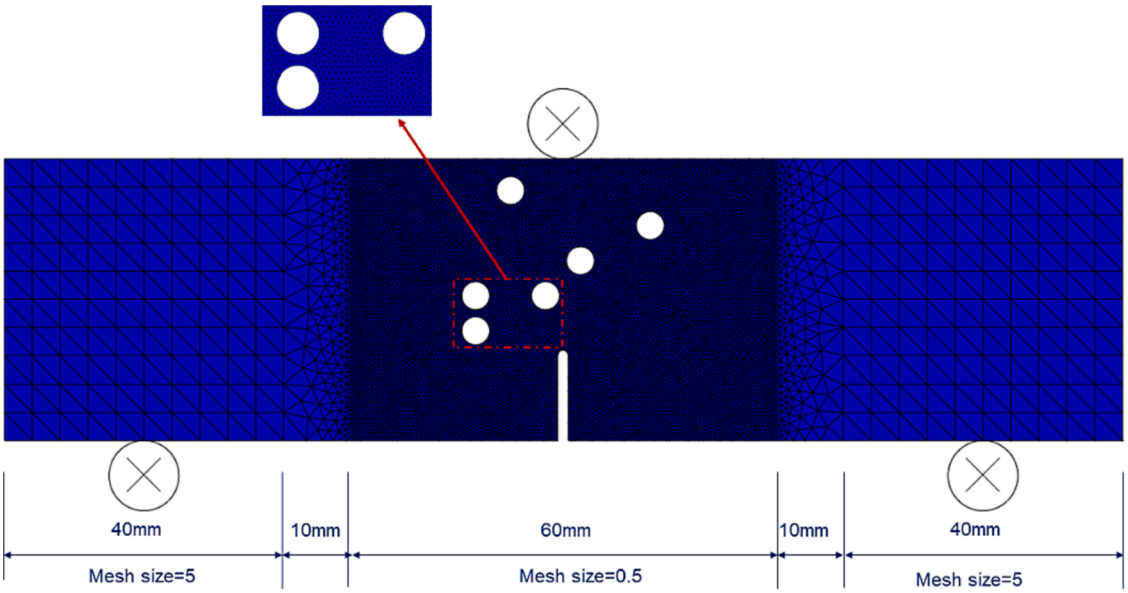

Fig. 3. Mesh size of the structure for numerical analyses in Abaqus.

Table 1
Input parameters for cementitious mortar .

(a) Compressive parameters of cementitious mortar	
Yield stress (MPa)	Inelastic strain (%)
38	0
45	0.005
1	0.015
(b) Tensile parameters of cementitious mortar	
Yield stress (MPa)	Cracking strain (%)
5.8	0
0.1	1

For convenience, a location is encoded as a 1 if there is a pore, otherwise it is encoded as a 0. In this way, one concrete structure could be encoded as a 5×8 matrix with elements of 0 or 1. Subsequently, the 5×8 matrix is flattened to a 40-dimensional vector, which is used as input for DNN model. The input representation can be found in Fig. 4(a).

As to the output representation, it is less complicated than the input since it is a scalar corresponding to the mechanical property we aim to optimize. To verify the feasibility of optimizing vascular structure of concrete for certain mechanical property with the data representation method, the target is first set as peak load, which can be directly obtained from the load–displacement curve. Afterwards, toughness, which is defined by the area below the load–displacement curve (Equation (4)), is used as the target to search for structures with more pores hit by the crack). One example of target representation could be seen in Fig. 4(b). Last, a hybrid target combining peak load and toughness are used to optimize vascular structure for self-healing concrete, the details will be illustrated in Section 3.3.1.

$$Toughness = \int_0^{0.2} Fds \tag{4}$$

Here F and s are load and displacement of the load–displacement curve, respectively.

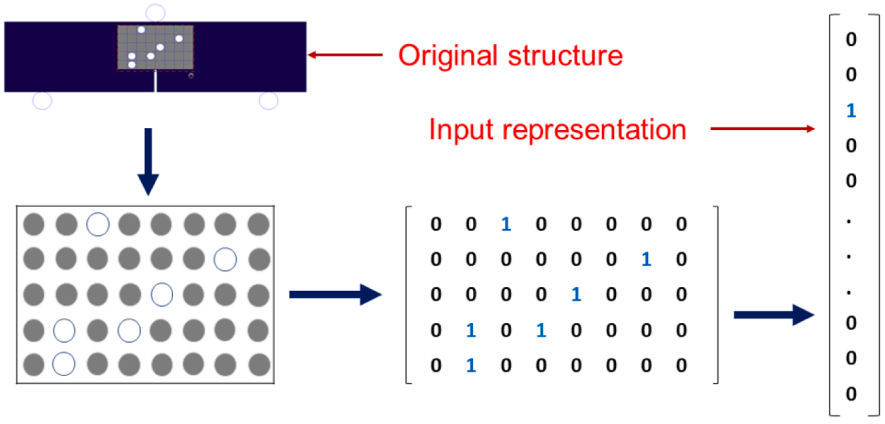

(a) Input representation

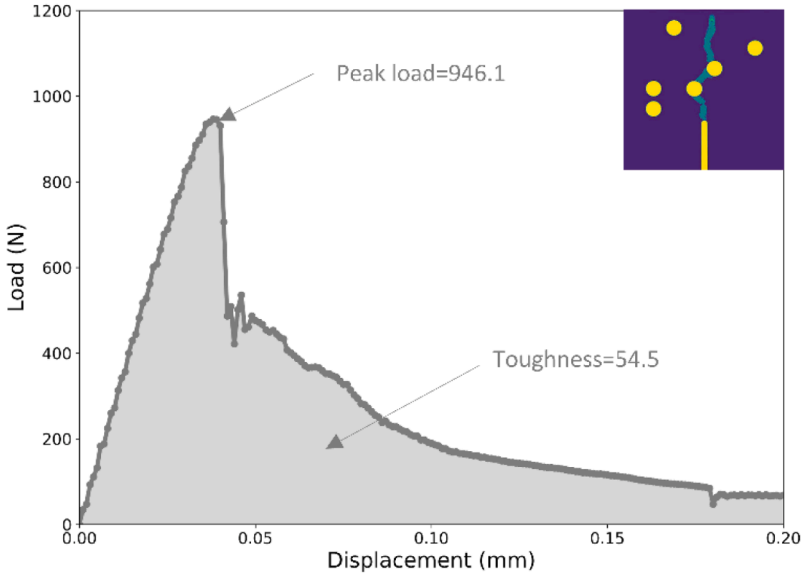

(b) Output representation

Fig. 4. Data representation (a) input representation (b) output representation.

2.2. Machine learning method

Artificial Neural Network (ANN) is a powerful algorithm for processing data by simulating the functioning of the biological neurons [34]. ANN uses linking functions to correlate features with targets. A deep neural network (DNN) is an ANN with multiple hidden layers. According to previous research [30], a deep network can represent functions of increasing complexity by adding more layers and more units within a layer. Theoretically, a neural network could approximate any function mapping from any finite dimensional discrete space to another. In this study, DNN with 6 hidden layers is established to predict the target property (peak load, toughness and hybrid target) based on the 40-dimensional vector representing the concrete structure. The number of neurons of the hidden layers is chosen as 512 for all hidden layers after hyperparameter tuning. A schematic of the DNN used is shown in Fig. 5.

The optimization method used here is similar to the research of Gu [28]. Two steps, i.e., weights (of DNN) training and input optimization, are used during the process. First, the weights of DNN are trained to map the input (vascular structure) to target (mechanical property) with the dataset. 10,000 vascular structures are randomly chosen and then calculated using numerical simulation (using Abaqus). The dataset is split with a split of 90–10 % between the training and test sets, i.e., trainset (size = 9,000) and test set (size = 1,000). The batch size is chosen as 512 after hyperparameter tuning. Coefficient of determination (R-squared) is selected as a metric to evaluate the accuracy of the ML models (Equation (5)). Mean squared error (MSE) is employed as the loss function (Equation (6)). Adam is used as the optimizer for the back-propagation with the default learning rate (0.001). ReLu function is employed as the activation function. The training process stops when the loss function is steady. The weights contributing to the highest R-squared on test set is saved.

$$R^2(y,y') = 1 - \frac{\sum (y_i - y_i')^2}{\sum (y_i - \bar{y})^2} \tag{5}$$

$$MSE = \frac{1}{n}\sum_{i=1}^{n}(y - y')^2 \tag{6}$$

After the DNN is well trained, the weights of the DNN are fixed while the input is set as the trainable variables to optimize input for higher mechanical property. To drive the DNN to search for the inputs with maximum target property, we define the negative of target as the loss function. During the optimization process, 20,000 inputs (40-dimensional vector) are randomly sampled from a Gaussian Distribution with expectation and variance of 6/40 and 0.3 respectively. The random initialization is to avoid the influence of initial exploration points. It is worth mentioning that we do not generate 'effective' inputs (only with 0′s or 1′s) because it spends more time for DNN to toggle the state of a location (from 0 to 1 or from 1 to 0) due to the small learning rate (0.001). Since the weights of the trained DNN are frozen, the back-propagation process will only drive the changes of input to minimize the loss function (higher mechanical property). Adam is also used as the optimizer for the back-propagation with the default learning rate (0.001) to accelerate the optimization process. 20,000 epochs are performed in this process since the loss function based on post-processed input keeps unchanged after that. The details can be found in Section 3.

The ML-optimized inputs need further post-processing after the optimization process. The learning rate is 0.001 and the elements after back-propagation are decimals, which fails to represent the position state (with/without pores). Therefore, it is necessary to convert the elements to binary value (0/1). In particular, we convert the positions with the top 6 maximum elements as 1′s and the rest as 0′s. This way, all the ML-recommended inputs are 40-dimensional vectors with six 1′s out of 40 positions. Then, the 40-dimensional vectors are reshaped 5×8 matrix and decoded into vascular structures. The schematics of the post-processing is shown in Fig. 6. Those ML-recommended structures are numerically verified with Abaqus software and their corresponding mechanical properties are re-calibrated. Finally, the vascular structure of concrete with highest target property is selected from the ML-recommended dataset and compared with the original dataset.

3. Results and discussion

3.1. Statistical properties of dataset

The load–displacement curve of the 10,000 samples in original dataset is shown in Fig. 7(a) and some randomly-chosen load–displacement curves along with the corresponding pore positions are given in Fig. 7(b). As shown in Fig. 7, the position of the 6 pores has a great influence on the mechanical response of the concrete structures, and it is necessary to design vascular structures for higher target mechanical properties by arranging these holes in different positions. Besides, it is found that the loads of most load–displacement curves are low when the displacement reaches 0.2 mm. In other words, most of the concrete structures fail when displacement is 0.2 mm. It is reasonable to calculate the toughness till displacement is 0.2 mm although it may be slightly overestimated for some structures which are extremely brittle.

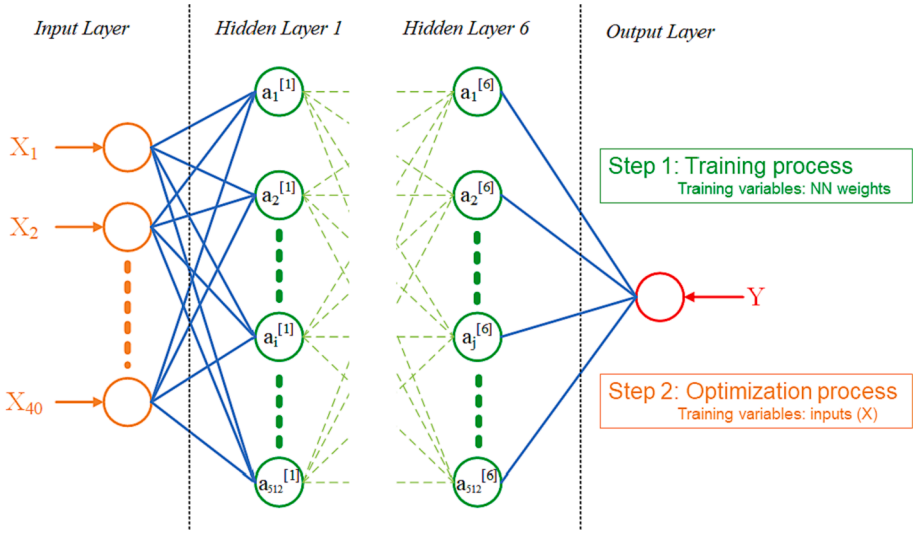

Fig. 5. General structure of a Deep Neural Network (DNN).

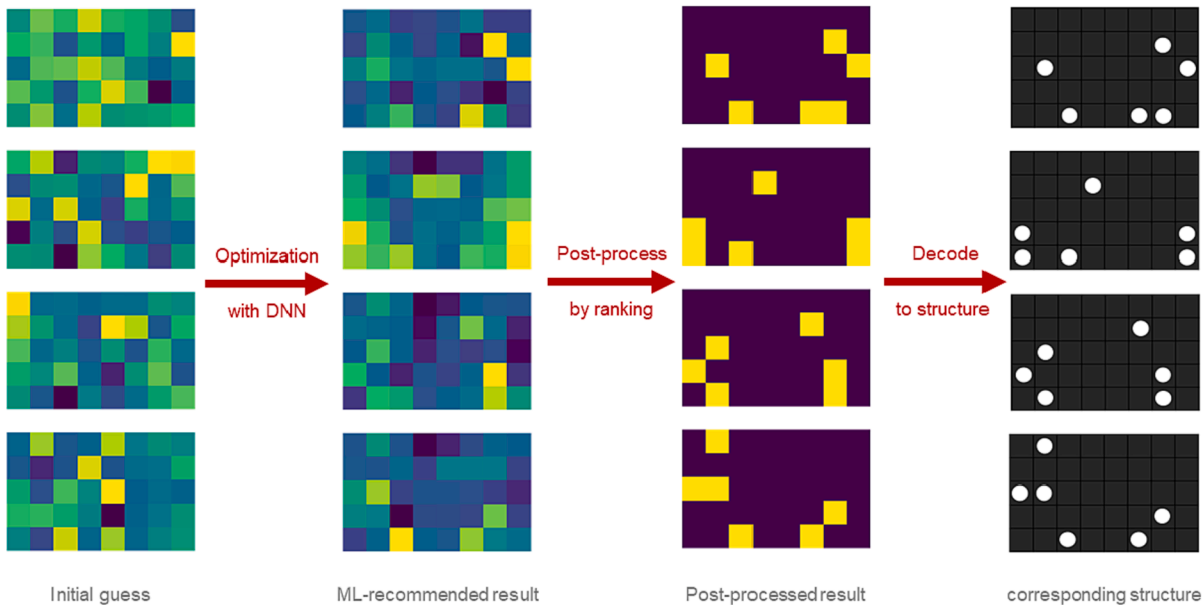

Fig. 6. Post-processing of ML-recommended input.

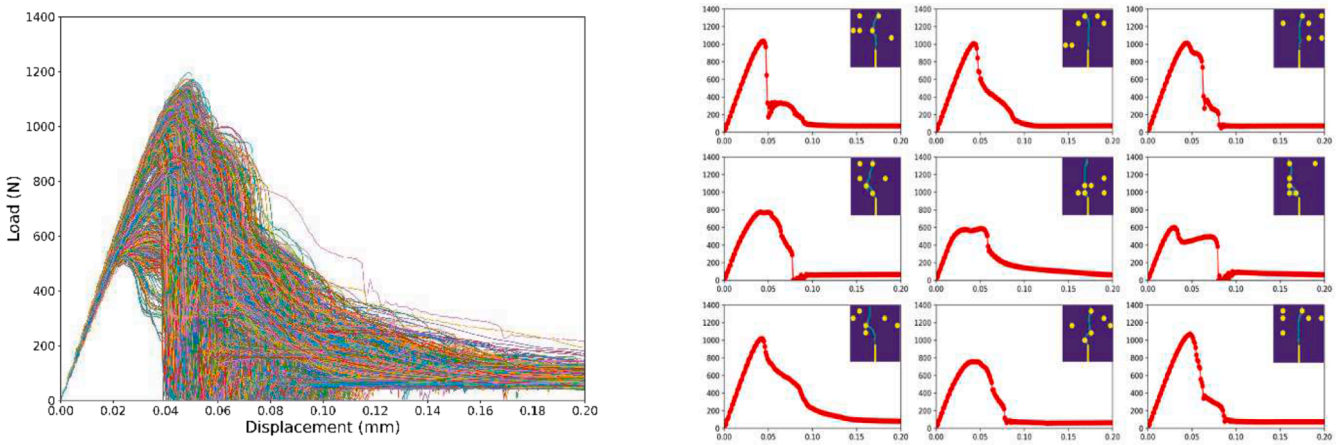

Fig. 7. Mechanical response of different vascular structures of concrete (a) displacement-load curve; (b) some examples of displacement-load curve and the corresponding structure.

The optimization targets are first set as peak load and toughness. The histograms of those two mechanical properties are shown in Fig. 8(a) and (b) respectively. The statistical properties of the targets are shown in Table 2. The maximum peak load and toughness are 1195.5 N and 97.2 N·mm respectively. Except for the vascular structures with 6 pores, the structure without pores is also numerically calculated as the reference. Based on Table 2, the highest toughness is much larger than the reference (55.5 N·mm). The largest peak load is slightly higher than the reference (1141.1 N), which may be caused by the simulation accuracy. The corresponding vascular structures with the highest peak load and the highest toughness are shown in Fig. 8(c) and 8(d) respectively. As shown in Fig. 8(c) and 8(d), the peak load of the concrete structure with highest toughness is low and vice versa. The vascular structure of concrete with highest peak load is more brittle than the structure with highest toughness. In addition, the crack hits less pores than that of the structure with highest toughness.

3.2. Optimization results of peak load and toughness

3.2.1. Optimization result of peak load

Peak load is relatively easy to predict because it could be directly obtained from the load–displacement curve. To seek for a vascular structure of concrete with higher peak load, a neural network is first trained to map the vascular structure to peak load. An accurate mapping relationship between input and output could make it easier to find the optimized structure. The prediction accuracy of the well-trained DNN model is shown in Fig. 9. It is obvious that the performance of the neural network model is remarkable with a R-squared of 0.963 on the test set.

After the DNN model is trained, 20,000 examples are randomly generated as initial guesses. To keep this process reproducible, the random seed is fixed to ensure that the same examples are generated in different runs. These examples are fed into the neural network and ran for 20,000 epochs. To illustrate the optimization process, the negative of average loss function (average peak load change) is presented to observe

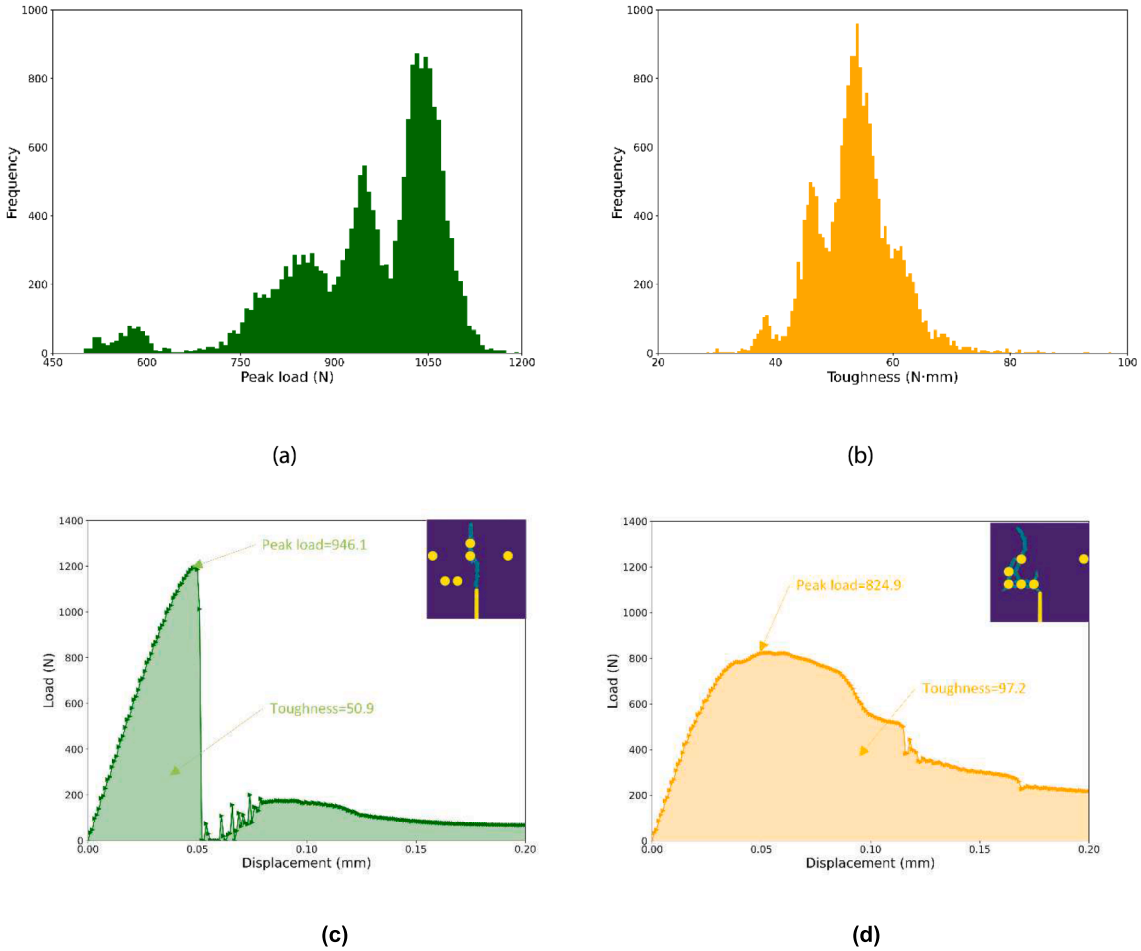

Fig. 8. (a) Histogram of peak load; (b) Histogram of toughness; (c) structure with the highest peak load; (d) structure with highest toughness.

Table 2
Statistical properties of the dataset.

	Peak load (N)	Toughness (N·mm)
Mean value	952.4	53.4
Standard deviation	123.1	6.8
Maximum value	1195.5	97.2
Minimum value	499.5	28.2
Reference	1141.1	55.5

the improvement of mean (predicted) peak load. The result is shown in Fig. 10. From Fig. 10, the average peak load dramatically increases in the first 2,000 epochs and keeps increasing steadily after 6,000 epochs. In other words, the initialized structures are optimized towards higher peak load. When analyzing the predicted result based on post-processed inputs (with 0/1), the initial average value is 952.5 N, which is almost the same with the mean value of the dataset (952.4 N). The average peak load after 20,000 epochs is 1123.6 N, which increases by 17.95 % from the initial guess (converted to 0/1). However, the value is lower than the

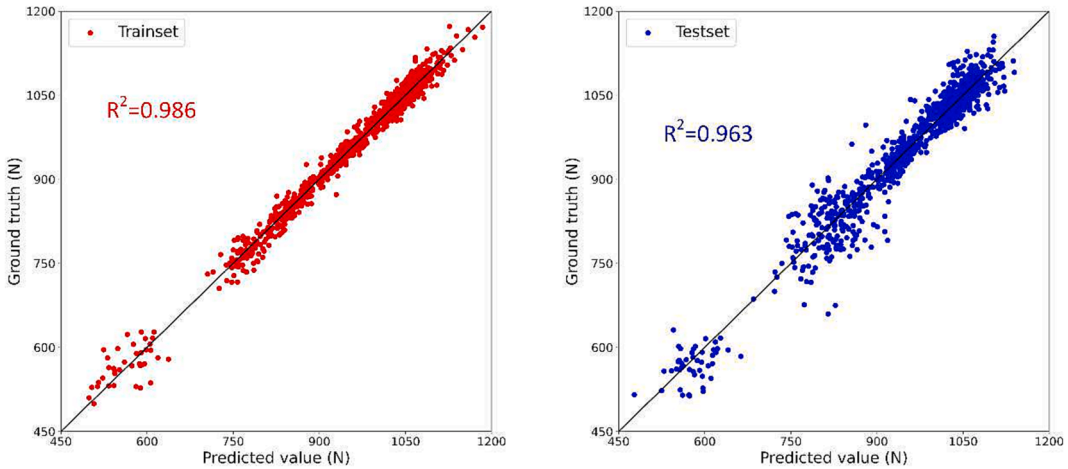

Fig. 9. Prediction accuracy of peak load.

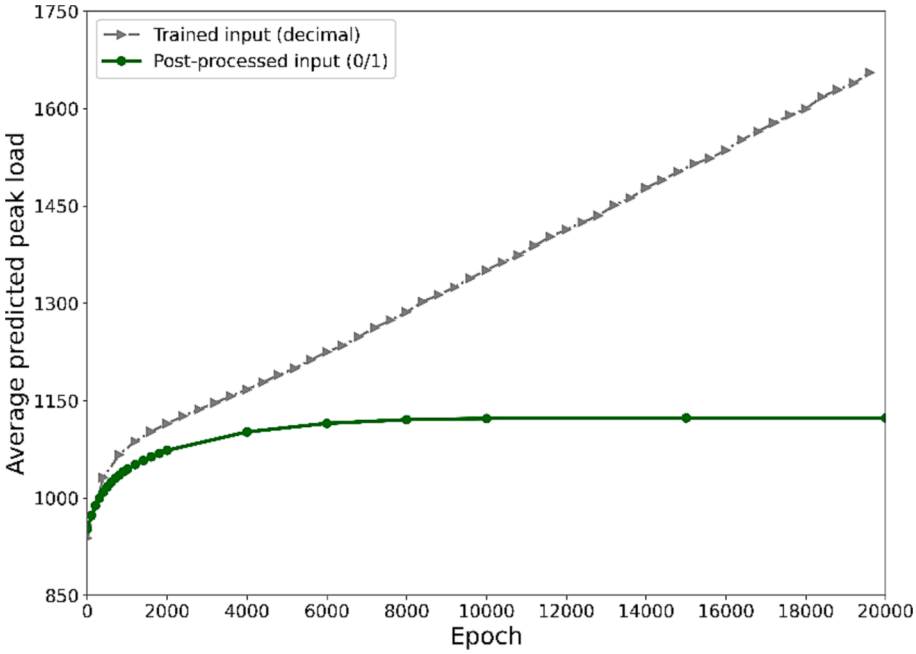

Fig. 10. Change of average peak load during optimization process.

ML-predicted average peak load with decimal inputs (1635.5 N) with a discrepancy of 42.81 %. But this does not affect the search for vascular structures with higher peak load since the 'effective' average peak load (predicted with post-processed input) increases. It is noted that the 'effective' average peak load remains almost steady after 10,000 epochs. Therefore, it is reasonable to stop the optimization process after 20,000 epochs even though the loss function continues to decrease.

As mentioned above, the ML-recommended results could not be directly used due to the decimal values of the inputs after optimization. To correctly describe the state of the positions, these results are converted into 0/1 by ranking the 40 values. Subsequently, those post-processed inputs are decoded into structures with 6 pores. It is found that the 20,000 initial structures converge to 870 unique vascular structures and those ML-recommended structures are numerically simulated to verified the peak load. The histogram of 20,000 ML-recommended structures is shown in Fig. 11.

From Fig. 11(a), it is noted that the overall peak loads of ML-recommended structures are higher than that of the original dataset. Therefore, the concrete structures improve for higher peak load after the optimization process using DNN. it is worth mentioning that the actual mean peak load of ML-recommended structures is 1117.3 N (increase by 17.31 %), which is very close to the model-predicted average value (1123.6 N). The DNN is still accurate when the dataset contains lots of structures with high peak load. As shown in Fig. 11(b), for the ML-optimized structures, only one crack occurs in most of them and it explains why these structures are with higher peak load. Among the optimized structures, the vascular structure of concrete with highest peak load is selected and the corresponding load–displacement curve (calculated in Abaqus) is shown in Fig. 12. As shown in Fig. 12, the peak load of the ML-recommended structure is 1197.5 N, which is an increase of 0.17 % from the concrete structure in the original dataset. For the ML-recommended vascular structure of concrete, the crack does not hit the pores, and this could explain why the structure is with the highest peak load than the other optimized structures. Clearly, while this is certainly optimal in terms of peak load, it is useless in terms of vascular-based self-healing: the self-healing can only be triggered if the crack hits a pore (i.e., the vascular).

3.2.2. *Optimization result of toughness*

Based on the result in 3.2.1, we found it feasible to optimize vascular

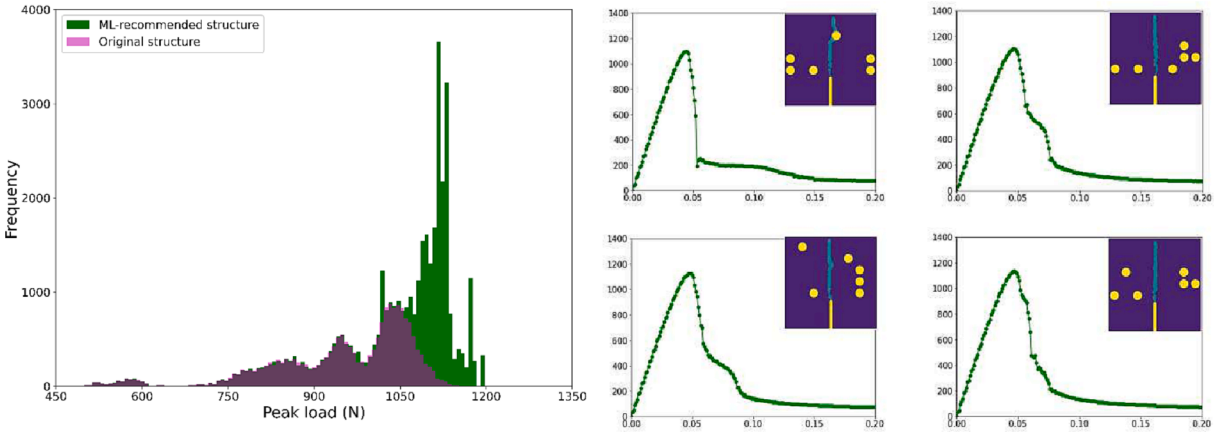

Fig. 11. ML-recommended structures for high peak load. (a) histogram of peak load of optimized structures; (b) some examples of displacement-load curve and the corresponding structure.

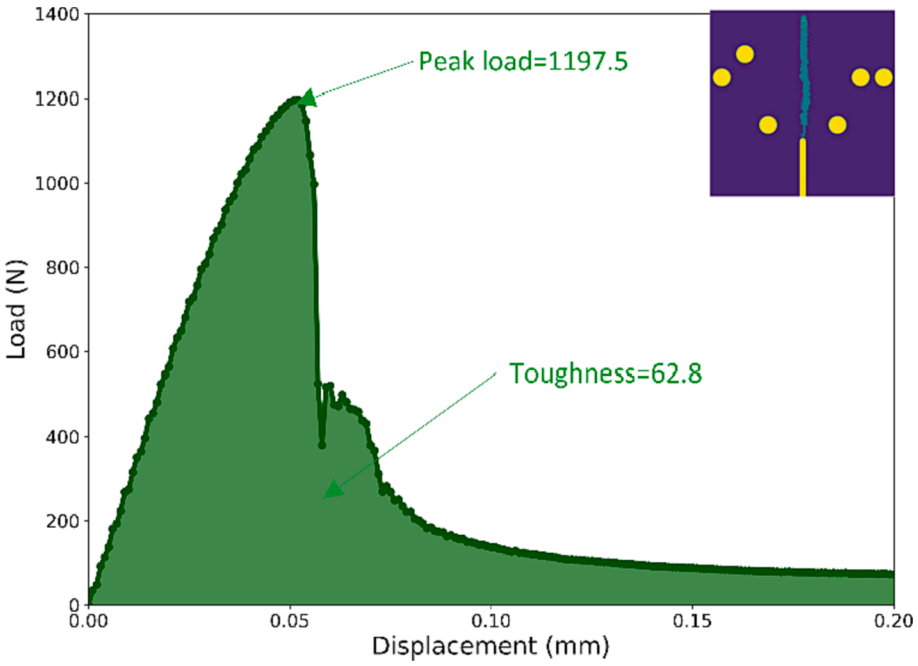

Fig. 12. ML-recommended structure with highest peak load.

structures of concrete towards higher peak load using the data representation method. Therefore, the neural network is re-trained to map the vascular structures to toughness, which is an indirect mechanical property calculated from displacement-load curve. The prediction accuracy of the well-trained DNN model is shown in Fig. 13. As shown in Fig. 13, the performance of the DNN model is still remarkable with a R-squared of 0.926 on test set. However, it is slightly poorer than the performance of the peak load one. One possible reason is that some structures fail before the displacement reaches 0.2 mm, which significantly overestimates the toughness. As a result, the target is less accurate than the peak load.

After the neural network is trained, 20,000 initial guesses are used as starting points for the optimization process. Similarly, these examples are fed into the DNN model and ran for 20,000 epochs. The negative of average loss function (average toughness change) is shown in Fig. 14. From Fig. 14, the average toughness increases during the optimization process, manifesting that the inputs changes towards higher toughness. The average (predicted) toughness based on post-processed input after 20,000 epochs is 71.8 N·mm. Compared with the result in peak load, the average toughness does not sharply increase in the first 2,000 epochs and spends more epochs (10,000 epochs) to reach the stable state. In addition, the difference between model-predicted toughness based on decimals input and post-processed input is much larger (233.15 %). Except for the binary transferring for input (covert result into 0/1), another possible reason is the inaccuracy of the ML model, especially when the toughness is high.

After post-processing and decoding the ML-recommended inputs into structures with 6-pores, the 20,000 initial structures converge to 5,959 unique structures after optimization, and those ML-recommended vascular structures of concrete are numerically simulated to verify their toughness. The histogram of 20,000 recommended structures is shown in Fig. 15.

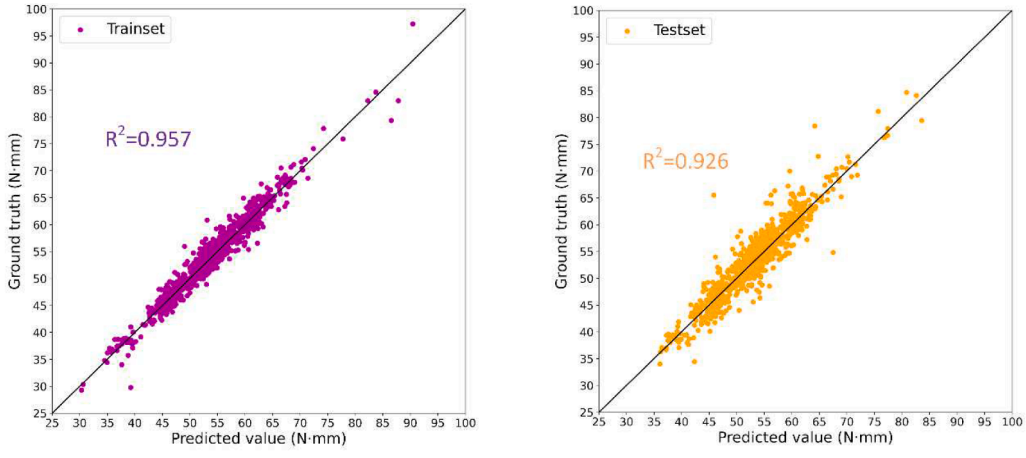

Fig. 13. Prediction accuracy of NN model for toughness on (a) training set; (b) test set.

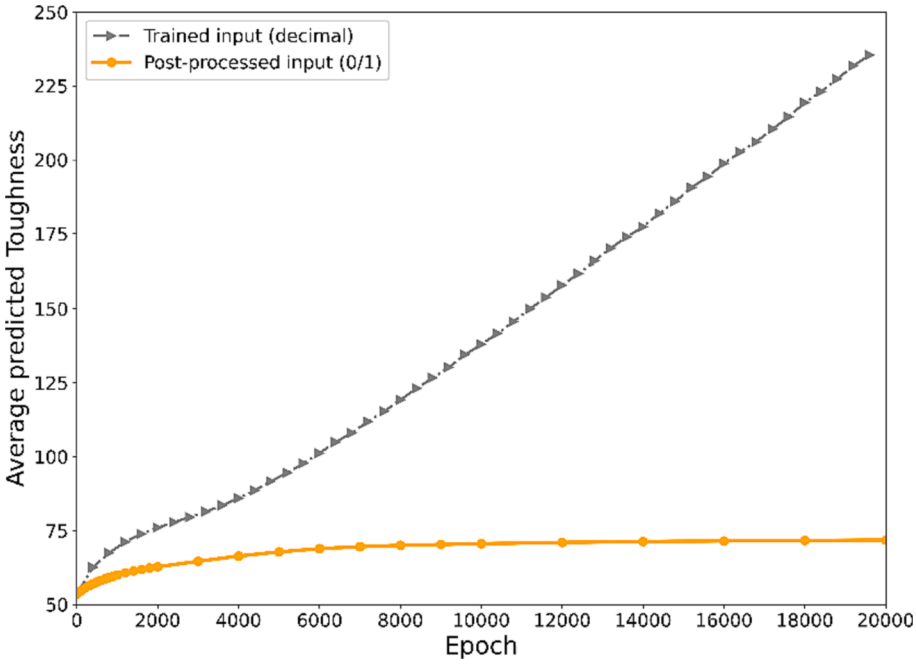

Fig. 14. Change of average toughness during training.

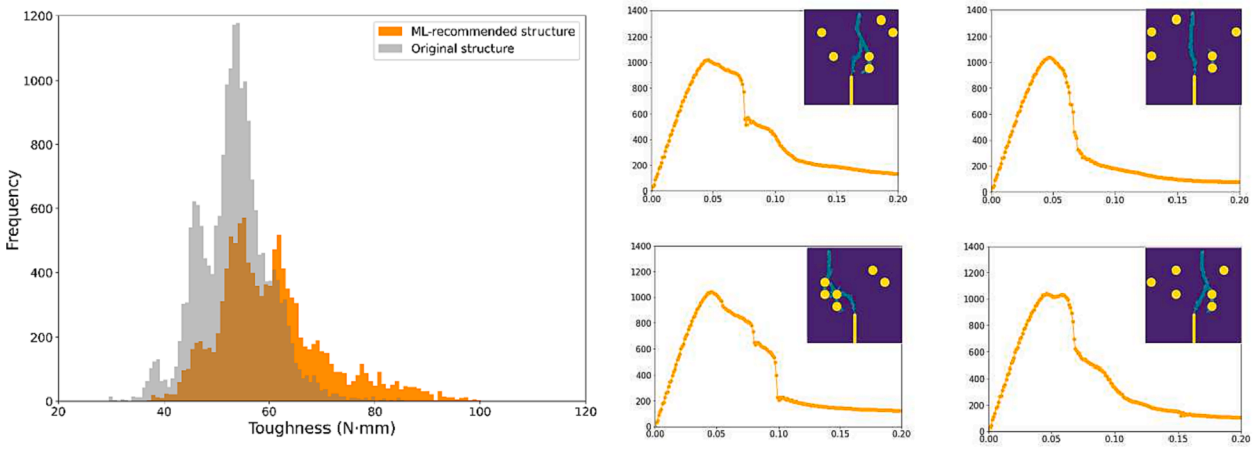

Fig. 15. ML-recommended structures for high toughness. (a) histogram of toughness of optimized structures; (b) some examples of displacement-load curve and the corresponding structure.

From Fig. 15, the overall toughness of the optimized structures is higher than that of the original dataset. The actual average toughness after optimization is 60.5 N·mm (increase by 13.17 %), which is smaller than the model-predicted value (71.8 N·mm). Unlike peak load, the distribution of toughness is with less variance and the samples with high toughness is much less in the training set. As a result, the DNN model becomes less accurate when the toughness is high. When looking into the optimized structures, multiple cracks occur in most of them and thereby inducing a higher toughness in Fig. 15(b). Among the optimized structures, the vascular structure of concrete with the largest toughness is found and the corresponding load–displacement curve is shown in Fig. 16. From Fig. 16, the ML-recommended structure has much higher toughness (111.0 N·mm) than the one in the original dataset, with an increase of 14.13 %. Compared with the original vascular structure, 4 pores of the optimized structure are hit/damaged by the crack, making the structure more ductile after the crack occurs. Meanwhile, 2 pores are far away from the crack and therefore the peak load is relatively larger than the original one. As a result, the toughness is much larger than the original vascular structure.

3.3. Optimization results for self-healing concrete

3.3.1. Define optimization target for self-healing concrete

After optimization towards higher peak load and toughness, a further investigation is carried out to optimize the vascular structure for self-healing purpose. To search for a structure suitable for self-healing concrete using DNN, the optimization target should first be defined. Two requirements need to be met: (1) The concrete is healable after cracked, and (2) The adverse influence of pores (vascular) on initial mechanical property should be minimized. For the first requirement, the crack must hit pores to make it healable. Considering the results from 3.2.2, the toughness of concrete structures tends to be high when cracks hit the holes. In other words, vascular structures of concrete with higher toughness could be regarded as more healable. Therefore, we describe the first part with toughness defined in this paper. Except for healable property, the adverse influence of pores on peak load should be

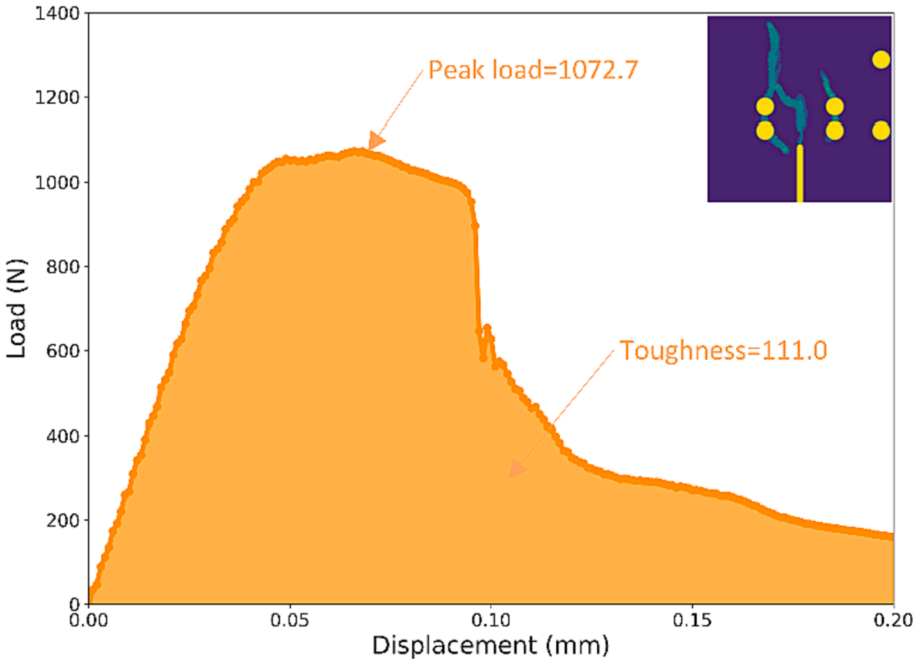

Fig. 16. ML-recommended structure with highest toughness.

minimized. To compromise between those two aspects, we defined the optimization target by a sum of the weighted toughness and peak load. In this paper, the hybrid-target (HT) used for self-healing concrete optimization is represented by Equation (7).

$$HT = \alpha T/T_{ref} + \beta P/P_{ref} \tag{7}$$

where$T$, P represent the toughness and peak load of concrete structure with 6 pores; α and β are the weight for toughness and peak load respectively;T_{ref},P_{ref} represent the toughness and peak load of the reference vascular structure (no pores) and they are also obtained by numerical simulation. For simplification, we assign equal importance to those two mechanical properties and$\alpha = \beta = 0.5$.

According to the definition above, the hybrid-target (HT) could be calculated. The distribution of the defined hybrid-target (HT) of the 10,000 samples in original dataset is shown in Fig. 17(a) and the concrete structure with highest HT is shown in Fig. 17(b).

As shown in Fig. 17, the mean value of hybrid target is about 0.899 and the distribution is quite different from that of peak load, which means that the influence of peak load is not as large as that of toughness. However, the vascular structure of concrete with the highest hybrid target is different from that of peak load or toughness. The two components (peak load and toughness) work together to search for the vascular structure instead of either single target. Therefore, it is necessary to design the vascular structure of concrete towards the hybrid target to considering those two aspects simultaneously.

3.3.2. *Optimization result of hybrid target*

To design vascular structure for self-healing concrete, the neural network is retrained to map the vascular structure to the defined hybrid target in advance. The prediction accuracy of the well-trained model is shown in Fig. 18. From Fig. 18, it is noted that the performance of the neural network model is still accurate with a R-squared of 0.896 on test set. It is much poorer than the DNN models for predicting peak load or toughness. The hybrid target combines both peak load and toughness and makes it somewhat more difficult for the neural network to learn.

Similarly, 20,000 examples (same with Section 3.2) are generated as initial guess for the optimization process. 20,000 epochs are carried out and the negative of average loss function (average hybrid target change) is shown in Fig. 19. From Fig. 19, the average HT dramatically increases in the first 2,000 epochs and steadily increases after that. The ‘effective’

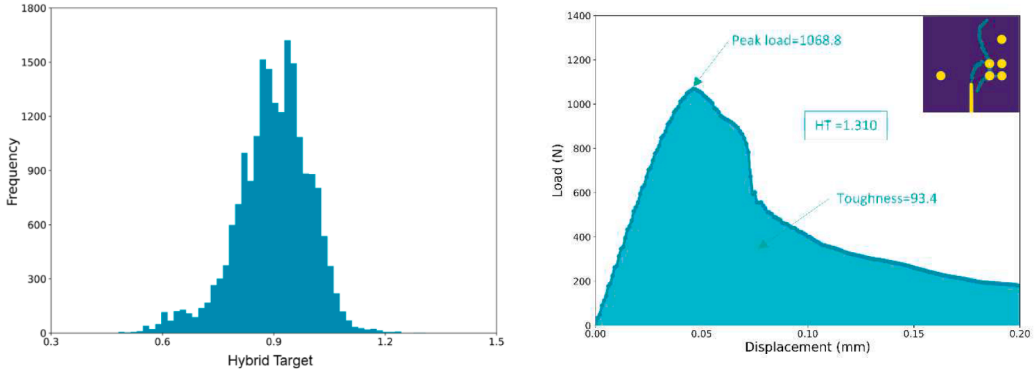

(a) (b)

Fig. 17. (a) Histogram of hybrid target; (c) structure with the highest hybrid target.

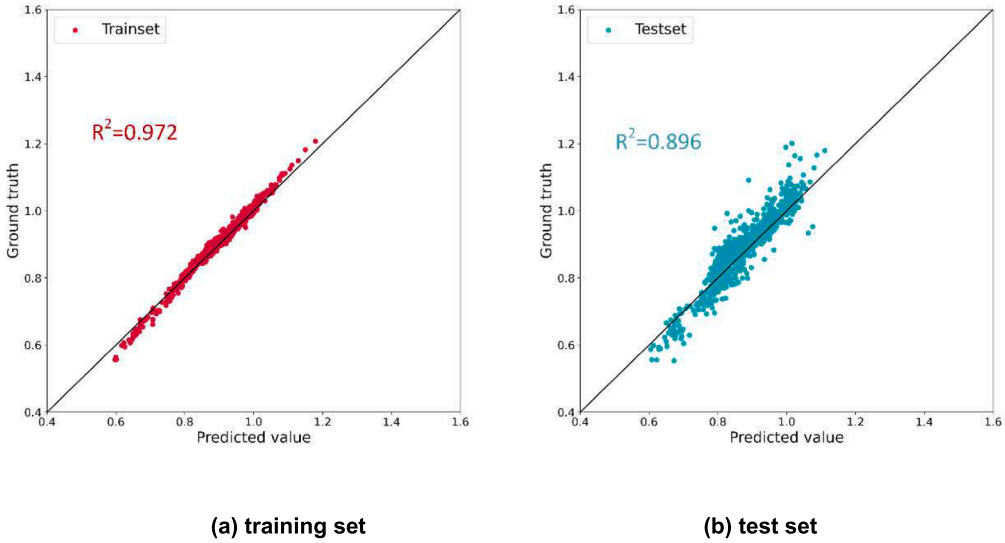

Fig. 18. Prediction accuracy of NN model for hybrid target on (a) training set; (b) test set.

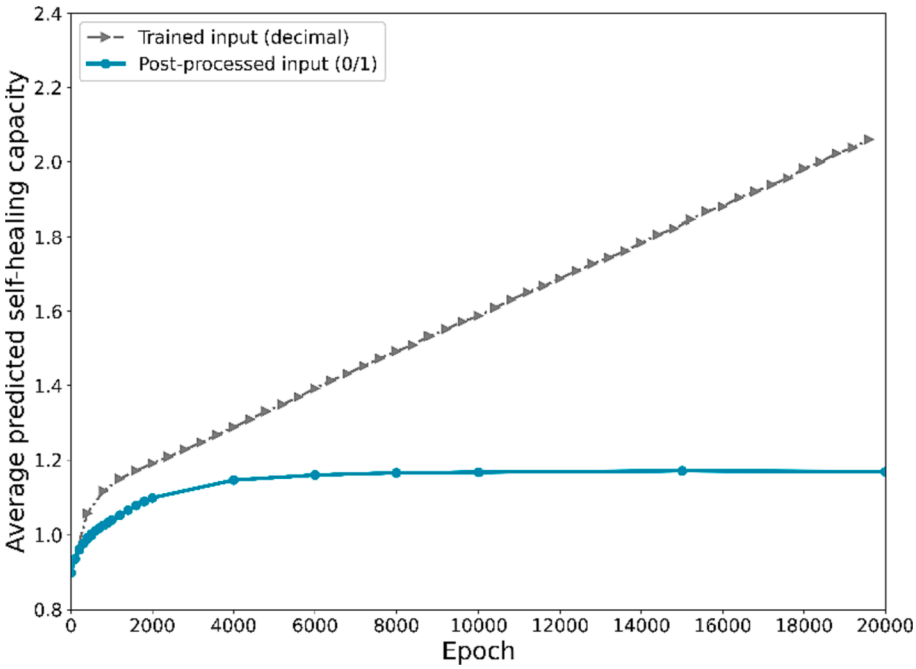

Fig. 19. Change of average toughness during training.

average HT based on post-processed input increases to 1.137 after 20,000 epochs. The difference between model-predicted toughness and 'effective' average is 82.17 %, which is between 42.81 % (peak load) and 233.15 % (toughness).

After converting the ML-recommended inputs into concrete structures with 6-pores, the 20,000 initial structures converge to 1,015 unique vascular structures of concrete and those ML-recommended structures are numerically simulated to verified the hybrid target. The histogram of 20,000 recommended structures is shown in Fig. 20. From Fig. 20, it is noted that the overall hybrid target of the optimized structures is higher than that of the original dataset after the optimization process using DNN. The actual average hybrid target increases by 9.51 % (0.984), which is much smaller than 1.137 due to the inaccurate DNN model.

Among the ML-optimized structures, the vascular structure with the highest hybrid target is selected and the corresponding load–displacement curve is shown in Fig. 21. From Fig. 21, the ML-recommended one has slight improvement (1.355) from the concrete structure with highest toughness in the original dataset (1.310). Compared with the original concrete structure, 4 pores of the optimized structure are hit/damaged by two cracks, resulting in an optimized structure with higher toughness (96.8 N·mm) than the original one (93.4 N·mm). Meanwhile, 2 pores are separately hit by the cracks instead of 3 pores hit by one crack in the original structure. As a result, the peak load is also higher (1100.8 N) than the original one (1068.8 N). Therefore, the ML-recommended structure has better self-healing capacity due to the fact that more pores are hit by crack while having a slightly increasing the peak load compared with the original structure.

Compared with the toughness, the improvement of the optimized structure is much smaller. The possible reason is that the third DNN

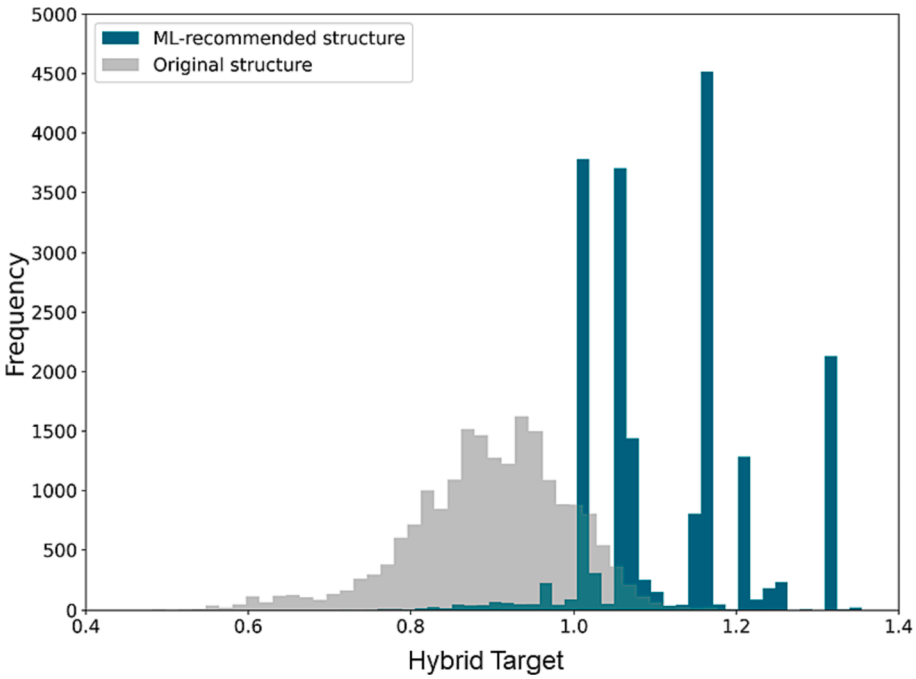

Fig. 20. Histogram of ML-recommended structures (hybrid target).

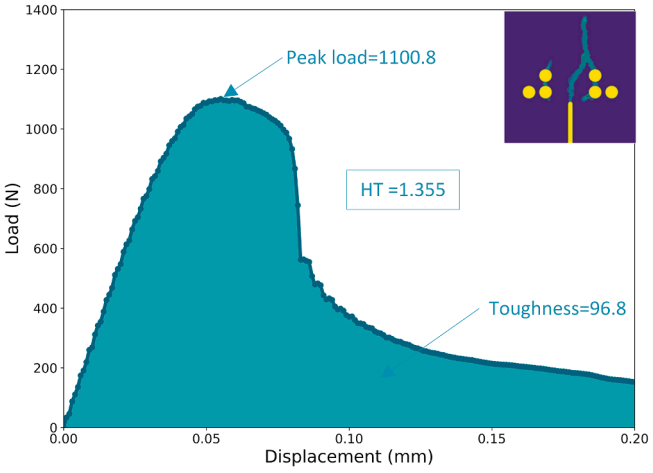

Fig. 21. ML-recommended structure with highest hybrid target.

model is less accurate, making it difficult to find a concrete structure as good as the second DNN model within 20,000 epochs. A possible solution is to increase the accuracy of the DNN model by training it with a larger dataset. Besides, it is noted that the weights for the two components could be tuned to look for a concrete structure suitable for self-healing concrete.

However, there are still a lot to do before the ML method could be used to the practical engineering. The case studied herein is a simplification: the notch induces a starting position of the crack, and the space above is used as a "design space". Different positioning of the voids will then be the major factor influencing the crack length and, thereby, the toughness. The simplified case is used to understand if the method proposed herein can be effectively utilized: the simplification allows the DNN model to accurately map the relationship between the structure and the target with a (relatively) limited amount of training data. Since this is shown to be possible, we believe that the optimization method could, in principle, be extended to real-life scenarios (but at a significantly higher computational cost).

4. Conclusion

In this work, vascular structure optimization towards different target mechanical properties was carried out using DNN. The optimization objective is a concrete beam with 6 pores out of 40 possible positions in the middle span representing vascular reservoirs for healing agent. To investigate the feasibility of using DNN to optimize vascular structure of concrete with the proposed data representation method, peak load and toughness are first set as the optimization target. Subsequently, a hybrid target is defined to optimize the vascular structure for self-healing concrete. Based on the presented results, the following conclusions can be drawn:

(1) According to the original 10,000 simulated examples, the position of the 6 pores has great influence on the mechanical response of the concrete beam. This necessitates the optimization of the vessel configuration for vascular-based self-healing concrete to achieve better mechanical properties.
(2) DNN model is able to accurately predict peak load, toughness as well as defined hybrid target based on concrete structures with the R-squared over 0.895 on the test set of the three ML models. However, the DNN models become less accurate when the target changes from direct mechanical property (peak load) to indirect mechanical property (toughness) and hybrid property.
(3) It is feasible to optimize vascular structure of concrete towards higher peak load, toughness and defined target by fixing the weights of the DNN model and training the input (the pores configuration). the average peak load, toughness and hybrid target of the ML-recommended concrete structure increase by 17.31 %, 34.16 % and 9.51 % after optimization.
(4) As to the highest target values among the ML-recommended structures, the targets increase by 0.17 %, 14.13 % and 3.45 % for peak load, toughness and self-healing concrete respectively. The ML-optimized vascular structures of concrete are different for the 3 individual scenarios. Therefore, it is necessary to simultaneously consider both peak load and toughness when designing concrete structure for self-healing purpose.
(5) Although concrete structure towards higher targets could be realized using DNN, the discrepancies between the ML-predicted

targets and the 'effective' average values based on post-processed input is 42.81 %, 233.15 % and 82.17 % for peak load, toughness and defined hybrid target respectively. This is caused by the different domains of input (concrete design space is discrete while the recommended input changes continuously) and the inaccuracy of DNN model.

CRediT authorship contribution statement

Zhi Wan: Conceptualization, Methodology, Data curation, Writing – review & editing. **Ze Chang:** Methodology, Writing – review & editing. **Yading Xu:** Conceptualization, Writing – review & editing. **Branko Šavija:** Supervision, Conceptualization, Methodology, Data curation, Writing – review & editing.

Declaration of Competing Interest

The authors declare that they have no known competing financial interests or personal relationships that could have appeared to influence the work reported in this paper.

Data availability

Data will be made available on request.

Acknowledgement

Zhi Wan and Ze Chang would like to acknowledge the financial support of the China Scholarship Council (CSC) under the grant agreement No.201906220205 and No.201806060129. Yading Xu and Branko Šavija acknowledge the financial support of the European Research Council (ERC) within the framework of the ERC Starting Grant Project "Auxetic Cementitious Composites by 3D printing (ACC-3D)", Grant Agreement Number 101041342.

References

[1] Rooij D, R. M, Schlange E. Self-healing phenomena in cement-based materials. Draft of State-of-the-Art Report of RILEM Technical Committee 221-SHC. 2011.
[2] K. Van Tittelboom, N. De Belie, D. Van Loo, P. Jacobs, Self-healing efficiency of cementitious materials containing tubular capsules filled with healing agent, Cem Concr Compos 33 (2011) 497–505, https://doi.org/10.1016/j.cemconcomp.2011.01.004.
[3] K. Van Tittelboom, N. De Belie, Self-healing in cementitious materials-a review, Materials (Basel) 6 (2013) 2182–2217, https://doi.org/10.3390/ma6062182.
[4] E. Tziviloglou, Z. Pan, H.M. Jonkers, E. Schlangen, Bio-based self-healing mortar: An experimental and numerical study, J Adv Concr Technol 15 (2017) 536–543, https://doi.org/10.3151/jact.15.536.
[5] B. Dong, G. Fang, Y. Wang, Y. Liu, S. Hong, J. Zhang, et al., Performance recovery concerning the permeability of concrete by means of a microcapsule based self-healing system, Cem Concr Compos 78 (2017) 84–96, https://doi.org/10.1016/j.cemconcomp.2016.12.005.
[6] C.M. Dry, Three designs for the internal release of sealants, adhesives, and waterproofing chemicals into concrete to reduce permeability, Cem Concr Res 30 (2000) 1969–1977, https://doi.org/10.1016/S0008-8846(00)00415-4.
[7] C.J. Hansen, W. Wu, K.S. Toohey, N.R. Sottos, S.R. White, J.A. Lewis, Self-healing materials with interpenetrating microvascular networks, Adv Mater 21 (2009) 4143–4147, https://doi.org/10.1002/adma.200900588.
[8] S. Sangadji, E. Schlangen, Self healing of concrete structures - Novel approach using porous network concrete, J Adv Concr Technol 10 (2012) 185–194, https://doi.org/10.3151/jact.10.185.
[9] Davies RE, Jefferson A, Lark R, Gardner D. A novel 2D vascular network in cementitious materials 2015.
[10] P. Minnebo, G. Thierens, G. De Valck, K. Van Tittelboom, B.N. De, D. Van Hemelrijck, et al., A novel design of autonomously healed concrete: Towards a vascular healing network, Materials (Basel) 10 (2017) 49, https://doi.org/10.3390/ma10010049.
[11] Z. Wan, Y. Xu, Y. Zhang, S. He, B. Šavija, Mechanical properties and healing efficiency of 3D-printed ABS vascular based self-healing cementitious composite: Experiments and modelling, Eng Fract Mech 267 (2022), 108471, https://doi.org/10.1016/J.ENGFRACMECH.2022.108471.
[12] K.-M. Wang, S. Lorente, A. Bejan, Vascularization with grids of channels: multiple scales, loops and body shapes, J Phys D Appl Phys 40 (2007) 4740, https://doi.org/10.1088/0022-3727/40/15/057.
[13] W. Zhang, Q. Zheng, A. Ashour, B. Han, Self-healing cement concrete composites for resilient infrastructures: A review, Compos Part B Eng 189 (2020), 107892, https://doi.org/10.1016/j.compositesb.2020.107892.
[14] O. Yerro, V. Radojevic, I. Radovic, M. Petrovic, P.S. Uskokovic, D.B. Stojanovic, et al., Thermoplastic acrylic resin with self-healing properties, Polym Eng Sci 56 (2016) 251–257, https://doi.org/10.1002/pen.24244.
[15] V.C. Li, Y.M. Lim, Y.W. Chan, Feasibility study of a passive smart self-healing cementitious composite, Compos Part B Eng 29 (1998) 819–827, https://doi.org/10.1016/S1359-8368(98)00034-1.
[16] H.R. Williams, R.S. Trask, I.P. Bond, Self-healing composite sandwich structures, Smart Mater Struct 16 (2007) 1198–1207, https://doi.org/10.1088/0964-1726/16/4/031.
[17] Z. Li, L.R. de Souza, C. Litina, A.E. Markaki, A. Al-Tabbaa, Feasibility of Using 3D Printed Polyvinyl Alcohol (PVA) for Creating Self-Healing Vascular Tunnels in Cement System, Materials (Basel) 12 (2019) 3872, https://doi.org/10.3390/ma12233872.
[18] K.S. Toohey, N.R. Sottos, J.A. Lewis, J.S. Moore, S.R. White, Self-healing materials with microvascular networks, Nat Mater 6 (2007) 581–585, https://doi.org/10.1038/nmat1934.
[19] A.R. Hamilton, N.R. Sottos, S.R. White, Self-healing of internal damage in synthetic vascular materials, Adv Mater 22 (2010) 5159–5163, https://doi.org/10.1002/adma.201002561.
[20] Y. Xu, H. Zhang, Y. Gan, B. Šavija, Cementitious composites reinforced with 3D printed functionally graded polymeric lattice structures: Experiments and modelling, Addit Manuf 39 (2021), 101887, https://doi.org/10.1016/j.addma.2021.101887.
[21] Z. Li, L.R. de Souza, C. Litina, A.E. Markaki, A. Al-Tabbaa, A novel biomimetic design of a 3D vascular structure for self-healing in cementitious materials using Murray's law, Mater Des 190 (2020), 108572, https://doi.org/10.1016/j.matdes.2020.108572.
[22] Z.L. Zhao, S. Zhou, K. Cai, X.Y. Min, A direct approach to controlling the topology in structural optimization, Comput Struct 227 (2020), 106141, https://doi.org/10.1016/J.COMPSTRUC.2019.106141.
[23] Y. Zhou, H. Zhan, W. Zhang, J. Zhu, J. Bai, Q. Wang, et al., A new data-driven topology optimization framework for structural optimization, Comput Struct 239 (2020), 106310, https://doi.org/10.1016/J.COMPSTRUC.2020.106310.
[24] R. Sivapuram, P.D. Dunning, H.A. Kim, Simultaneous material and structural optimization by multiscale topology optimization, Struct Multidiscip Optim 54 (2016) 1267–1281, https://doi.org/10.1007/S00158-016-1519-X/FIGURES/18.
[25] K. Guo, Z. Yang, C.-H. Yu, M.J. Buehler, Artificial intelligence and machine learning in design of mechanical materials, Mater Horizons 8 (2021) 1153–1172, https://doi.org/10.1039/d0mh01451f.
[26] C. Qiu, S. Du, J. Yang, A deep learning approach for efficient topology optimization based on the element removal strategy, Mater Des 212 (2021), 110179, https://doi.org/10.1016/J.MATDES.2021.110179.
[27] Y.C. Hsu, C.H. Yu, M.J. Buehler, Tuning Mechanical Properties in Polycrystalline Solids Using a Deep Generative Framework, Adv Eng Mater 23 (2020) 2001339, https://doi.org/10.1002/adem.202001339.
[28] C.-T. Chen, G.X. Gu, Generative Deep Neural Networks for Inverse Materials Design Using Backpropagation and Active Learning, Adv Sci 7 (2020) 1902607, https://doi.org/10.1002/ADVS.201902607.
[29] F. Sui, R. Guo, Z. Zhang, G.X. Gu, L. Lin, Deep Reinforcement Learning for Digital Materials Design, ACS Mater Lett (2021) 1433–1439, https://doi.org/10.1021/acsmaterialslett.1c00390.
[30] Y. Lecun, Y. Bengio, G. Hinton, Deep learning, Nat 2015 (5217553) (2015.436–44.) 521, https://doi.org/10.1038/nature14539.
[31] V.Chaudhari S, A. Chakrabarti M. Modeling of Concrete for Nonlinear Analysis using Finite Element Code ABAQUS. Int J Comput Appl 2012;44:14–8. 10.5120/6274-8437.
[32] Heaton J. An empirical analysis of feature engineering for predictive modeling. Conf Proc - IEEE SOUTHEASTCON 2016;2016-July. 10.1109/SECON.2016.7506650.
[33] Z. Wan, Y. Xu, B. Šavija, On the use of machine learning models for prediction of compressive strength of concrete: Influence of dimensionality reduction on the model performance, Materials (Basel) 14 (2021) 1–23, https://doi.org/10.3390/ma14040713.
[34] Verhaegh WFJ, Aarts E, Korst J, editors. Algorithms in Ambient Intelligence 2004; 2. 10.1007/978-94-017-0703-9.